Measurements of Velocity, Velocity Fluctuation, Density, and Stresses in Chute Flows of Granular Materials

Hojin Ahn
Assoc. Mem. ASME

Christopher E. Brennen
Mem. ASME

Rolf H. Sabersky
Mem. ASME

California Institute of Technology,
Pasadena, CA 91125

Experiments on continuous, steady flows of granular materials down an inclined channel or chute have been conducted with the objectives of understanding the characteristics of chute flows and of acquiring information on the rheological behavior of granular material flow. Two neighboring fiber-optic displacement probes provide a means to measure (1) the mean velocity by cross-correlating two signals from the probes, (2) the unsteady or random component of the particle velocity in the longitudinal direction by a procedure of identifying particles, and (3) the mean particle spacing at the boundaries by counting the frequency of passage of the particles. In addition, a strain-gauged plate built into the chute base has been employed to make direct measurement of shear stress at the base. With the help of these instruments, the vertical profiles of mean velocity, velocity fluctuation, and linear concentration were obtained at the sidewalls. Measurements of some basic flow properties such as solid fraction, velocity, shear rate, and velocity fluctuation were analyzed to understand the characteristics of the chute flow. Finally, the rheological behavior of granular materials was studied with the experimental data. In particular, the rheological models of Lun et al. (1984) for general flow and fully developed flow were compared with the present data.

1 Introduction

Recent theoretical research has added greatly to our knowledge of the rheological behavior of rapidly flowing granular materials. For example, Ogawa et al. (1980), Savage and Jeffrey (1981), Jenkins and Savage (1983), and Lun et al. (1984) have led to a comprehension of how stresses and solid fraction in a granular flow are related to velocity gradient and to the kinetic energy associated with random motions of particles (the so-called granular temperature). Moreover, for simple shear flow, all the theoretical analyses predict a rheological behavior which is a natural extension of that originally proposed by Bagnold (1954). Namely,

$$\tau_{ij} = \rho_p f_{ij}(\nu) d^2 \left(\frac{du}{dy}\right)^2$$

where τ_{ij} is the stress tensor, ρ_p is the density of the solid particle, f_{ij} is a tensor function of solid fraction, ν, d is the diameter of the particle, and du/dy is the local mean shear rate. Lun et al. (1984) estimated the ratio of the characteristic mean shear velocity, $d(du/dy)$, to the root mean square of velocity fluctuations to be a function only of solid fraction and the coefficient of restitution. In their analysis the velocity fluctuations were assumed to be isotropic. Furthermore, the effect of a variable coefficient of restitution which depends on the particle impact velocity, has been studied by Lun and Savage (1986). It has been found that the coefficient of restitution, which increases with decreasing impact velocity, causes the stresses to vary with the shear rate to a power less than two.

These advances have been greatly aided by computer simulations (for example, Campbell and Brennen (1985a,b), Walton and Braun (1986a,b), Campbell and Gong (1986), and Campbell (1989)). Especially Walton and Braun (1986b), Campbell and Gong (1986), and Campbell (1989) produced results similar to those of the theoretical models. However, velocity fluctuations are found to be anisotropic. That is, as solid fraction decreases, granular temperature deviates from an isotropic distribution. The effect of a variable coefficient of restitution has also been examined in the computer simulation by Walton and Braun (1986b). The results manifested a deviation from those of the constant coefficient of restitution in a manner similar to that of Lun and Savage (1986), but the calculated stresses were significantly lower than those of ex-

Contributed by the Applied Mechanics Division of THE AMERICAN SOCIETY OF MECHANICAL ENGINEERS for publication in the JOURNAL OF APPLIED MECHANICS.

Discussion on this paper should be addressed to the Technical Editor, Leon M. Keer, The Technological Institute, Northwestern University, Evanston, IL 60208, and will be accepted until two months after final publication of the paper itself in the JOURNAL OF APPLIED MECHANICS. Manuscript received by the ASME Applied Mechanics Division, Apr. 17, 1989; final revision, Sept. 12, 1990.

perimental studies and Lun and Savage. Though there has been significant success, computer simulation faces difficulties in creating realistic boundary conditions. In addition, complicated interactions between particles and between solid walls and particles remain to be explored.

On the other hand, progress in experimental methods for granular materials has been very limited, being hindered by the obvious difficulties involved in making point measurements of velocity, solid fraction, or granular temperature in the interior of granular material flow. For example, granular temperature, in spite of its importance, had not been experimentally measured until Ahn et al. (1988) used fiber-optic displacement probes to measure one component of velocity fluctuations. The present state of the experimental information on granular material flows consists of a number of Couette flow studies (e.g., Savage and McKeown (1983), Hanes and Inman (1985), and Craig et al. (1986)) and several studies of flows down inclined chutes (e.g., Bailard (1978), Augenstein and Hogg (1978), Patton et al. (1987), and Ahn et al. (1988)). Understandably, the initial objective of some of the Couette flow experiments (such as those of Savage and McKeown (1983)) was to produce a simple shear flow with uniform velocity gradient, uniform solid fraction, and hopefully, uniform granular temperature. To this end the surfaces of the solid walls were roughened to create a no-slip velocity condition at the wall. Practical engineering circumstances require the knowledge of how to model the conditions for smooth walls at which slip occurs. This presents some difficulties because the boundary conditions on the velocity and granular temperature at the smooth walls are far from clear (see, for example, Campbell (1988)).

Chute flows differ from Couette flows and have a "conduction" of granular temperature as indicated in Campbell and Brennen (1985b). In their work, a boundary layer next to the wall had a lower solid fraction and higher granular temperature than the bulk further from the wall, indicating a conduction from the boundary layer to the bulk. Granular conduction has more extensively been studied by Ahn et al. (1989). The results show that granular temperature can be conducted either from the wall boundary to the free surface, or from the free surface to the wall, depending on the values of the coefficient of restitution and the angle of chute inclination. Furthermore, the granular conduction term and the dissipation term are found to be comparable in magnitude. The results also show a significant role played by the granular conduction in determining the profiles of granular temperature, solid fraction, and velocity.

This paper contains a study of continuous, steady flows of granular materials down an inclined chute. The objective was to understand the characteristics of granular chute flows and to acquire information on the rheological behavior of granular flow.

2 Review of Rheological Models

In this section, the existing rheological models postulated by Lun et al. (1984) will be reviewed for the purpose of analyzing the present experimental data. Comparisons between simple shear flow and fully developed chute flow will also be included.

For two-dimensional flow which is steady and fully developed in the flow direction, the translational fluctuation energy equation is given as follows (see, for example, Jenkins and Savage (1983)):

$$-P_{yx}\frac{du}{dy}-\frac{\partial q_y}{\partial y}-\gamma=0, \tag{1}$$

where P_{yx} is the shear stress, u is the velocity in the flow direction, y is a coordinate in the direction normal to the flow, and q_y is the y-component of fluctuation energy flux. The rate of the dissipation of fluctuation energy per unit volume is denoted by γ. The first term is the work done to the system by stresses, and the second term represents the conduction of the fluctuation energy.

Following Lun et al., the normal and shear stresses and the dissipation term are given as follows:

$$P_{yy}=\rho_p g_1(\nu,e_p)T, \tag{2}$$

$$P_{yx}=-\rho_p g_2(\nu,e_p)d\frac{du}{dy}T^{1/2}, \tag{3}$$

$$\gamma=\frac{\rho_p}{d}g_3(\nu,e_p)T^{3/2}, \tag{4}$$

where ρ_p is the density of the solid particle, and d is the diameter of the particle. The granular temperature, T, is defined by $1/3\ (\langle u'^2\rangle+\langle v'^2\rangle+\langle w'^2\rangle)$ where u', v', and w' are three velocity fluctuation components. And $g_1(\nu,e_p)$, $g_2(\nu,e_p)$, and $g_3(\nu,e_p)$ are functions of solid fraction, ν, and the particle-particle coefficient of restitution, e_p.

For simple shear flow with uniform density and granular temperature, the conduction term in the energy equation (1) vanishes. Therefore, the shear work term and the dissipation term should balance. Using equation (1) with (3) and (4), the ratio of the characteristic velocity gradient to the granular temperature is obtained as follows:

$$S=\frac{d\dfrac{du}{dy}}{T^{1/2}}=\left(\frac{g_3}{g_2}\right)^{1/2}. \tag{5}$$

Note that S is a function only of ν and e_p. Therefore, (2) and (3) can be written as follows:

$$P_{yy}=\rho_p\left(d\frac{du}{dy}\right)^2\frac{g_1 g_2}{g_3}, \tag{6}$$

$$P_{yx}=\rho_p\left(d\frac{du}{dy}\right)^2\frac{g_2^{3/2}}{g_3^{1/2}}. \tag{7}$$

The ratio of shear stress to normal stress, or friction coefficient, is also a function only of ν and e_p.

On the other hand, fully developed chute flow does not have uniform temperature and solid fraction over the depth of the flow. Therefore, the conduction term remains in the energy equation (1) and it plays an important role in determining the profiles of granular temperature, solid fraction, and velocity (see Ahn et al. (1989)). Simple momentum principles are sufficient to demonstrate that for fully developed chute flow, the ratio of shear stress to normal stress is a constant given by tan θ where θ is the angle of chute inclination. From (2) and (3), therefore, S is given by

$$S=\frac{d\dfrac{du}{dy}}{T^{1/2}}=\frac{g_1}{g_2}\tan\theta. \tag{8}$$

It should be noted that S is a function not only for ν and e_p but also of tan θ. And since ν varies over the depth of the chute flow, S also varies, tending to zero at the free surface. Under these circumstances, (2) and (3) can be written as

$$P_{yy}\tan^2\theta=\rho_p\left(d\frac{du}{dy}\right)^2\frac{g_2^2}{g_1}, \tag{9}$$

$$P_{yx}\tan\theta=\rho_p\left(d\frac{du}{dy}\right)^2\frac{g_2^2}{g_1}. \tag{10}$$

These characteristics of chute flows will be important in considering the results presented in this paper.

3 Experimental Measurements

The present experiments were conducted in a long rectangular aluminum channel or chute—7.62 cm wide and 1.2 m

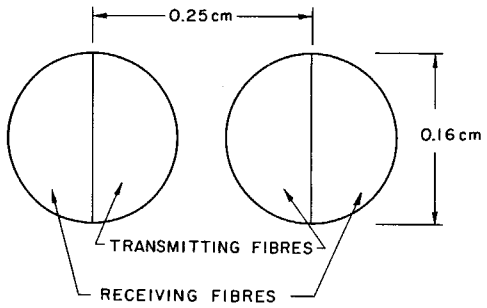

Fig. 1 Geometry of the faces of the two displacement probes used for velocity measurements with the 1.26-mm diameter glass beads

long. The chute was installed in a continuous flow, granular material facility, as previously described in Patton et al. (1987). The material enters the chute from an upper hopper and is collected in a collecting hopper from which, in turn, a mechanical conveyor delivers the material to the upper hopper. The channel is positioned at different angles, θ, to the horizontal. Measurements were taken only after a steady-state flow had been established. The flow into the channel is regulated by a vertical gate, and the opening between the gate and the channel base is referred to as the entrance gate height, h_o.

In these experiments two sizes of glass beads were used as granular materials; one is of mean diameter $d = 1.26$ mm with 2.9 percent standard deviation, and the other has $d = 3.04$ mm with 7.2 percent standard deviation. The maximum shearable solid fraction, ν^* was estimated from measurements of the values for the two cases in which the materials are densely packed and loosely packed in a container. The 1.26-mm beads had a value of $\nu^* = 0.61$. For the 3.04 mm beads, ν^* is 0.59. The density of both granular materials is $\rho_p = 2500$ kg/m^3.

Two important instruments were used in the experiments; one is a gauge to measure shear stress, and the other is a set of two fiber-optic probes to measure mean velocity and velocity fluctuation. In order to measure shear stress of flowing material at the chute base, a rectangular hole, 11.4 cm long and 3.8 cm wide, was cut into the chute base and replaced by a plate supported by strain-gauged flexures sensitive to the shearing force applied to the plate. Calibration of this balance was achieved by placing weights on the plate with the channel set at various inclinations. The clearance between the plate and the rest of the chute base was adjusted to be about 0.2 mm, much smaller than the particle sizes. Nevertheless, dirt would occasionally get trapped in the gap and this necessitated cleaning of the gap prior to each measurement.

A system of fiber-optic probes, similar to that originally devised by Savage (1979), was developed to measure particle velocities and their fluctuations at the chute base, the free surface, and the sidewalls. The system consisted of two MTI fiber-optic displacement probes set with their faces flush in a lucite plug which was, in turn, either set flush in the chute base or sidewalls or held close to the free surface of the flowing granular material. The probe faces were 1.6 mm in diameter and of the type in which one semicircle of the face consisted of transmitting fibers and the other of receiving fibers. The specific geometry is shown in Fig. 1. The distance between two displacement probes was selected to be about two particle diameters. This distance was carefully calibrated by placing the probes close to a revolving drum to which particles had been glued, and comparing the drum peripheral velocity with the velocity measured from the probe output.

The output from these velocity measuring devices was processed in the following way. First, the signals from each of the two displacement probes were simultaneously digitized and stored using a data acquisition system. Sampling rate was varied, depending on the mean velocity of particles. For most flows, the record time was about 0.5 second, recording at 3×10^4 samples/sec. Typically, each record detected the passage of 300 ~ 600 particles. The two records were digitally cross-correlated over the entire record in order to obtain the mean particle velocity, u. This information was then used to identify the peaks on the two records corresponding to the passage of a particular particle. When no such correspondence could be established or where the peak was below a certain threshold, the data was discarded for the purposes of this second part of the analysis. However, where positive identification was made, the velocity of that individual particle was obtained from the time interval between the peaks it generated on the two records. In this way, a set of instantaneous particle velocities were obtained, and ensemble-averaging was used to obtain both the mean velocity, u, and the root mean square of velocity fluctuation, u'. Though the latter represents only one component of velocity fluctuations, it should be some measure of granular temperature. Finally, the number of particle passages per unit time detected by the probe was divided by the mean velocity to obtain the characteristic particle spacing, C_{1D}, and in turn the linear concentration, ν_{1D}, was calculated as $\nu_{1D} = d/C_{1D}$ where d is the mean diameter of the particles. An estimate of the local solid fraction near the wall, ν_w, was calculated using $\nu_w = \pi \nu_{1D}^3/6$.

In addition, point probes were used to record the depth, h, of flow at several longitudinal locations in the channel. Mass flow rate, $\dot{m}$, was obtained by timed collection of material discharging from the chute. Mean velocities at the chute base and at the free surface obtained by the fiber-optic probes were averaged to give the average mean velocity, u_m, over the depth of the flow. A mean solid fraction, ν_m, could then be obtained as $\nu_m = \dot{m}/\rho_p h b u_m$ where b is the channel width. Furthermore, mean shear rate was calculated as $\Delta u/h$ where Δu is the difference between the two velocities at the base and at the free surface, and h is the depth of the flow. Normal stress was calculated by $\tau_N = \rho_p \nu_m g h \cos\theta$ where g is the gravitational acceleration, and shear stress, τ_S, was measured directly by the shear gauge. All the above measurements except for shear stress were made at two stations located at 72 cm and 98 cm downstream from the entrance gate. The shear gauge was located in the middle of these two stations. It should be noted that ν_w, u, u', τ_N, and τ_S are local properties while ν_m and $\Delta u/h$ represent quantities averaged over the depth of flow. The data from all the measurements were quite repeatable, and the data presented here are typically averages over two or five measurements.

Preliminary tests suggested that the flow could be influenced by the surface conditions of the chute base. Indeed, the data were quite sensitive to the degree of the cleanliness of the aluminum chute base. Therefore, it was possible to create different surface conditions with the aluminum chute by controlling the cleanliness. In addition, a very thin film of liquid rubber (Latex) was applied to the chute base to give a totally different surface condition. This film was about 0.2 mm thick. Before conducting experiments, the chute was run long enough to achieve a steady-state surface condition. With these precautions, data will be classified in this presentation by whether the chute base was "smooth," "moderately smooth," or "rubberized." The state of being moderately smooth was quite stable, but the smooth surface condition was less stable, requiring careful control of the cleanliness. To systematically characterize these different surface conditions, Coulombic friction coefficients were measured using the shear gauge and a block to which glass beads were glued. The kinematic Coulombic friction coefficient of the smooth surface was 0.15; the moderately smooth and rubberized surface had coefficients of 0.22 and 0.38, respectively. Furthermore, smooth and moderately smooth surfaces yielded coefficients of restitution different from that of the rubber-coated surface; the former was 0.7 while the latter 0.5. Both were measured by observing an

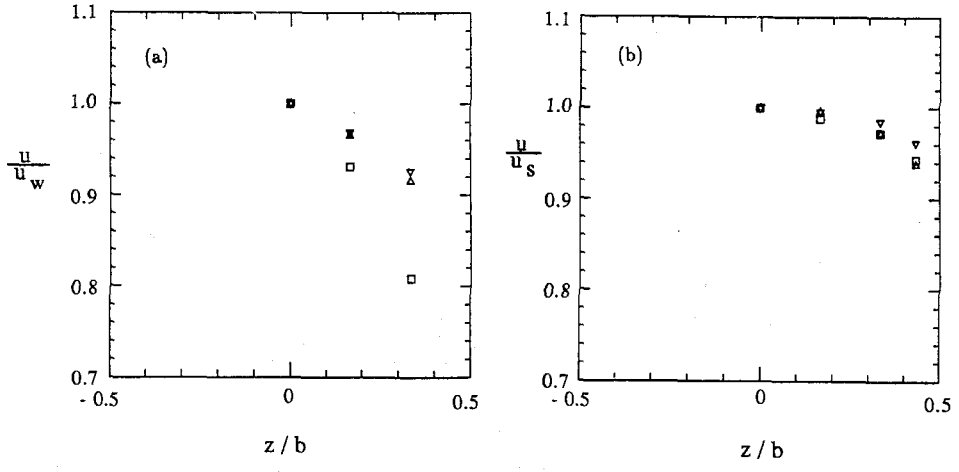

Fig. 2 The transverse velocity profiles (a) at the chute base and (b) at the free surface; mean velocity normalized by mean velocity at the center against the lateral location, z, normalized by the chute width, b = 76.2 mm. □, θ = 17.8 deg, ν_m = 0.54, u_w = 0.898 m/sec, and u_s = 1.118 m/sec; Δ, θ = 22.7 deg, ν_m = 0.50, u_w = 1.386 m/sec, and u_s = 1.639 m/sec; ▽, θ = 32.2 deg, ν_m = 0.49, u_w = 2.055 m/sec, and u_s = 2.263 m/sec. u_w, velocity at the center on the chute base; u_s, velocity at the center on the free surface.

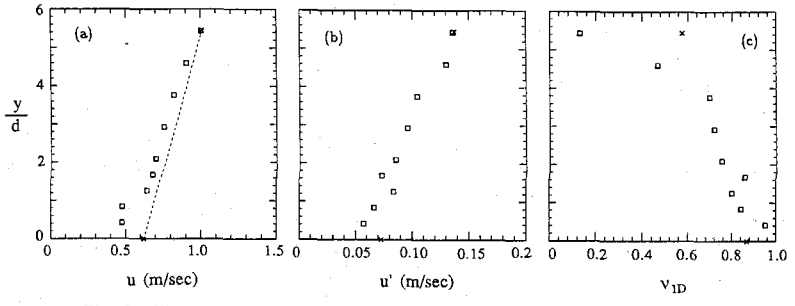

Fig. 3 The vertical profile at the sidewall, □. Vertical location, y, normalized by the particle diameter d against (a) mean velocity, (b) velocity fluctuation, and (c) linear concentration. ×, data at the center of the chute. Dotted line, the assumed velocity profile at the center of the chute. Data were taken at θ = 17.8 deg on the rubberized surface; ν_m = 0.30, h_o = 25.4 mm, and d = 3.04 mm.

individual particle colliding with the surface. These coefficients of restitution, e_w, between the wall surface and a particle should be distinguished from that between two particles, e_p, which was not measured here.

4 Preliminary Observations on Profiles

Originally the chute was designed to be wide enough to yield almost two-dimensional flow. To examine the effect of the sidewalls (and the extent to which this objective was achieved), fiber-optic probe measurements were made at several lateral locations with various chute inclinations. The 1.26-mm glass beads were used in measurements of the transverse velocity profiles, and the surfaces of the aluminum chute base as well as the sidewalls were smooth. Velocities normalized by the velocity at the centerline are plotted in Fig. 2. Comparison of the profiles on the free surface and on the chute base indicates that the flow at the free surface is more uniform and less affected by sidewall than the flow at the base. This is a "corner effect" in which particles in the corner are slowed both by the chute base and the side wall. One could visually observe that particles in the corner are arranged in a distinct line which has high solid fraction and low velocity. It should also be noted from Fig. 2 that the higher the velocity (or the higher the chute inclination), the less significant the sidewall effect. Thus nonuniformity, due to the sidewall, was significant only at the base and at low velocities (low inclinations). We were particularly concerned about the sidewall effect on the shear gauge whose width was one half of that of the channel. The foregoing results indicated that this sidewall effect would be very small.

Vertical profiles were obtained by making measurements through lucite windows in the sidewalls. Savage (1979) made similar efforts to obtain velocity profiles at the sidewalls using fiber-optic probes. Bailard (1978) obtained the vertical profiles of velocity and solid fraction by measuring cumulative mass flux profiles. Campbell and Brennen (1985b) in the computer simulation with circular discs obtained the profiles of velocity, granular temperature, and solid fraction. In the present work, fiber-optic probes were used to measure velocity, its fluctuation, and linear concentration. It should be noted that, usually, fully developed flow could not be achieved because of the finite length of the chute.

One typical example of the vertical profiles is included in Fig. 3, the measurements being taken with 3.04-mm glass beads with a chute inclination of 17.8 deg and a rubberized chute base. As illustrated in Fig. 3(*a*), the velocity profile is fairly linear except within a distance of about one particle diameter from the base. The uniform velocity within the distance of one-particle diameter indicates that there is a distinct layer at the corner, preventing particles from entering the layer from above, assuring the existence of the "corner effects." Note that the ratio of velocity at the base to that at the free surface

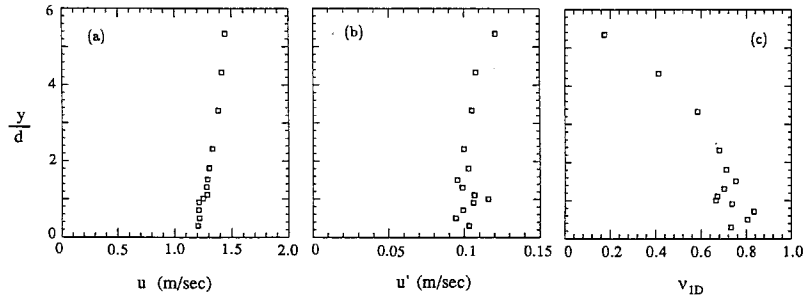

Fig. 4 The vertical profile at the sidewall, □. Vertical location, y, normalized by the particle diameter d against (*a*) mean velocity, (*b*) velocity fluctuation, and (*c*) linear concentration. Data were taken at $\theta = 22.7$ deg on the smooth surface; $h_o = 15.9$ mm and $d = 1.26$ mm.

is about one half, which is comparable with the results of the computer simulation by Campbell and Brennen (1985b). This result should be distinguished from those of Savage (1979) and Bailard (1978) where almost zero velocity was obtained at the chute surfaces roughened by rough rubber sheets or attached particles.

Velocities at the center of the chute, both at the base and the free surface, are shown in Fig. 3(*a*) for comparison with the velocities at the sidewall. At the free surface, the velocities at the center and at the sidewall are almost equal. But at the base there is some discrepancy due to the corner effect. This characteristic of the data suggests that the velocity profile in the center of the chute is similar to that at the sidewall except within one particle diameter distance from the base. An assumed velocity profile at the center is shown by the dotted line in Fig. 3(*a*). We also conclude from these observations that the shear rate, du/dy, can be approximated by the difference between the base and free-surface velocities, Δu, divided by the depth, h, of the flow. This approximation has been used throughout the analysis which follows.

The profile of velocity fluctuations at the sidewall is plotted in Fig. 3(*b*). It can be seen that the profile is fairly linear, and that fluctuations are larger at the free surface than at the chute base. Comparison between the sidewall and center values is also included in Fig. 3(*b*). At the free surface, no significant difference is encountered between the velocity fluctuations at the sidewall and at the center. But at the base, a small discrepancy is observed which is again believed to be due to the corner effect. This fairly linear profile for velocity fluctuation was observed in most flows. Furthermore, the fluctuations were always higher at the free surface than at the base of the chute. These overall features are in contrast to the results obtained by Campbell and Brennen (1985b). In their computer simulation, granular temperature near the solid wall was substantially higher than near the free surface, and the profile was far from linear. We believe this difference is probably due to that fact that 0.6 was used for e_p in the computer simulation, while e_p for glass beads is more like 0.95 (Lun and Savage (1986); refer to Ahn et al. (1989) for more detail).

When Fig. 3(*b*) is closely examined, it raises some complicated problems in measurements of granular flows. For instance, a slight peak in the velocity fluctuation was consistently observed at a distance of one-particle diameter from the chute base. This location coincides with the interface between the first and second layers of particles which are quite distinct because of the corner effect. Within each distinct layer, the fiber-optic probes measure only longitudinal fluctuations for the particles within that layer. At the interface, however, particles from both layers contribute, and hence the difference in the mean velocities in the two layers enters into the result. Therefore, the fluctuations at the interface were observed to be slightly higher than elsewhere.

The profile of linear concentration, ν_{1D}, is presented in Fig. 3(*c*). Again, in the region near the base, the locations of the first and second layers and their interface can be determined by the details of the profile. The peak at $y/d \simeq 0.5$ indicates the location of the center of the first layer; the interfacial region has a lower concentration; the peak at $y/d \simeq 1.7$ corresponds to the center location of the second layer. This detailed structure seems to disappear above the second layer. Near the free surface, the linear concentration decreases gradually, and as a result the free surface is not clearly defined as it might otherwise be.

The monotonic decrease of solid fraction with distance from the wall as shown in Fig. 3(*c*) was a somewhat unexpected result. From previous experiments (Bailard (1978)) and from computer simulations (Campbell and Brennen (1985b)), it has been observed that solid fraction increases with distance from the base and it vanishes at the free surface after it achieves its maximum in the bulk. The discrepancy between the profile of the present experiments and the results of Bailard may be due to the different surface conditions used in the experiments. The experiments of Bailard used the surface on which particles were glued to create a no-slip condition at the boundary. On the other hand, the present experiments used relatively smooth surfaces. The discrepancy between the present data and the results of Campbell and Brennen may arise from the fact that the value of e_p used by Campbell and Brennen is different from that of the glass beads in the present experiments. The results of Ahn et al. (1989) show that the profile of solid fraction can be either of Campbell and Brennen or of the present one, depending on the value of e_p.

Similar sidewall measurements were made with other sizes of glass beads and at other chute inclinations (Ahn (1989)); the general features of these profiles are similar to those of the preceding example though the data with a smooth aluminum base differed somewhat from that with the rubberized base. To illustrate this, measurements with the 1.26-mm glass beads at a chute inclination of 22.7 deg with the smooth aluminum base are presented in Fig. 4. Compared to the data on the rubberized surface, the profiles of velocity and velocity fluctuation are more uniform. The velocity at the wall is more than 80 percent of that at the free surface. Velocity fluctuation is fairly uniform, although there is a slight increase with distance from the chute base. The detailed structure of the layers due to the corner effect is clearly observed in all the profiles.

5 Presentation of Experimental Data

5.1 Experimental Data on Basic Flow Properties. In this section, we examine how basic flow properties (such as velocities, velocity fluctuation, and shear rate) vary with solid fraction. Two kinds of solid fraction are used in this presentation; mean solid fraction, ν_m, and wall solid fraction, ν_w. The mean solid fraction is an average value over the depth of flow, and the wall solid fraction describes a density in the vicinity of the

chute base. Because it is calculated from a measurement of linear concentration, the wall solid fraction may not represent accurately the local solid fraction near the wall, but it is at least a qualitative, comparative measure.

The ratio of velocity at the wall, u_w, to velocity at the free surface, u_s, is plotted against mean solid fraction in Fig. 5. Different symbols are used for different surface conditions. For the smooth surface, the ratio u_w/u_s is fairly constant and greater than 0.9, implying that the velocity profile over the depth is close to uniform. On the other hand, for the rubberized surface, the ratio increases with decreasing ν_m. In other words, the lower the solid fraction, the more uniform the velocity profile. Note the rather sudden change of u_w/u_s at $\nu_m \simeq 0.1$ which will be discussed later. As expected, the data for the moderately smooth surface lie between those for the smooth surface and the rubberized surface.

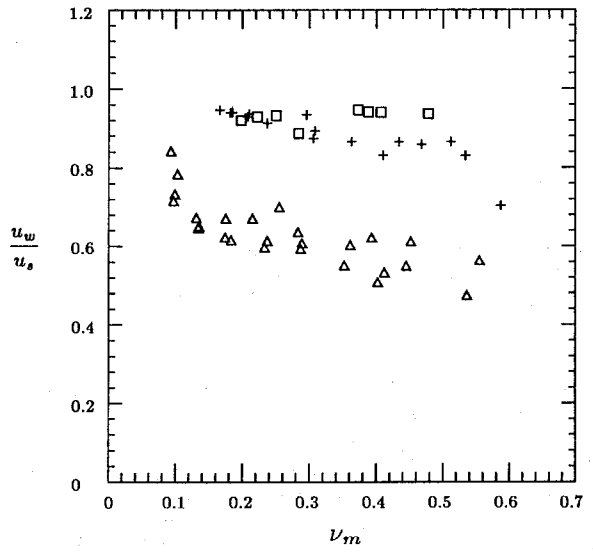

Fig. 5 The ratio of velocity at the chute base wall to velocity at the free surface, u_w/u_s, against mean solid fraction, ν_m. □, the smooth surface, +, the moderately smooth surface; Δ, the rubberized surface.

The mean shear rate, $\Delta u/h$, is plotted against mean solid fraction in Fig. 6. For the smooth surface (see Fig. 6(*a*)), the shear rate monotonically increases with decreasing ν_m. (Recall, however, u_w/u_s remains constant as shown in Fig. 5). On the other hand, the moderately smooth and rubberized surfaces (see Figs. 6(*b*) and (*c*)) yield shear rates which first increase and then decrease as the solid fraction decreases. The values of ν_m at which the shear rate is a maximum are about 0.3 for the moderately smooth surface, and about 0.2 for the rubberized surface regardless of the particle size. Note that the steep change of the shear rate at $\nu_m \simeq 0.1$ for the rubberized surface corresponds to that of u_w/u_s in Fig. 5.

The variation of the velocity fluctuation at the wall, u'_w, with wall solid fraction is examined in Fig. 7(*a*). Regardless of surface conditions, u'_w increases with decreasing ν_u. The use of wall solid fraction was essential for the examination of the local quantity u'_w. To illustrate this, the local quantity u'_w was plotted against the mean quantity ν_m as shown in Fig. 7(*b*). The use of the mean quantity with the local quantity leads to a wide scattering of the data. If examined more closely, the data reflected a strong dependency on the entrance gate opening h_o. As observed in Fig. 7(*b*), the data have a distinct line for each h_o. This is because the mean solid fraction is closely related to h_o. Note that fully developed flow was not achieved in the present experiments (this will be discussed later). Therefore, the test section was directly affected by entrance conditions governed by h_o. When ν_w is used, the dependency on h_o largely disappears as shown in Fig. 7(*c*).

It is also interesting to present the velocity fluctuation in a nondimensionalized form. In Fig. 8, the velocity fluctuation normalized by the mean velocity is plotted against wall solid fraction. Note all the quantities are local values measured at

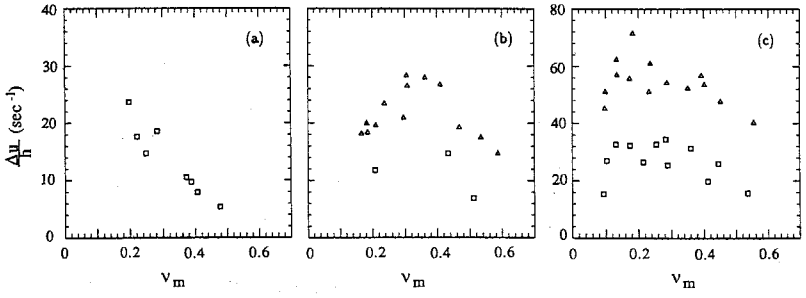

Fig. 6 The shear rate, $\Delta u/h$, against mean solid fraction, ν_m: (*a*) the smooth surface, (*b*) the moderately smooth surface, and (*c*) the rubberized surface. □, $d = 3.04$ mm; Δ, $d = 1.26$ mm.

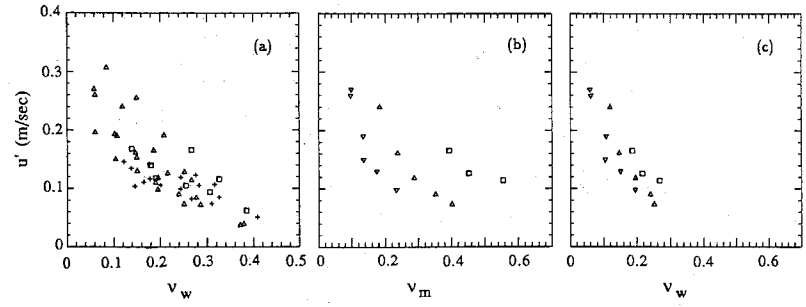

Fig. 7 The longitudinal velocity fluctuation at the wall, u'_w, against solid fraction with the rubberized surface. (*a*) Data for $d = 1.26$ mm and $d = 3.04$ mm. □, the smooth surface; +, the moderately smooth surface; Δ, the rubberized surface. (*b*) Data for $d = 1.26$ mm. □, $h_o = 38.1 \sim 50.8$ mm; Δ, $h_o = 25.4$ mm; ▽, $h_o = 12.7 \sim 15.9$ mm. (*c*) Data as in (*b*).

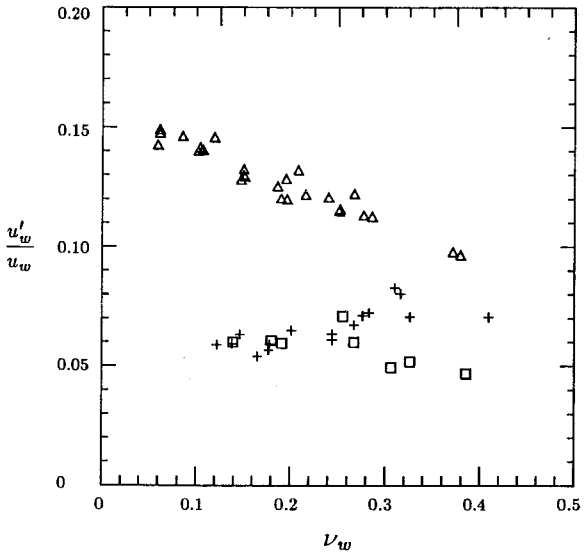

Fig. 8 The longitudinal velocity fluctuation at the chute base wall normalized by mean velocity, u'_w/u_w, against wall solid fraction, ν_w. □, the smooth surface; +, the moderately smooth surface; Δ, the rubberized surface.

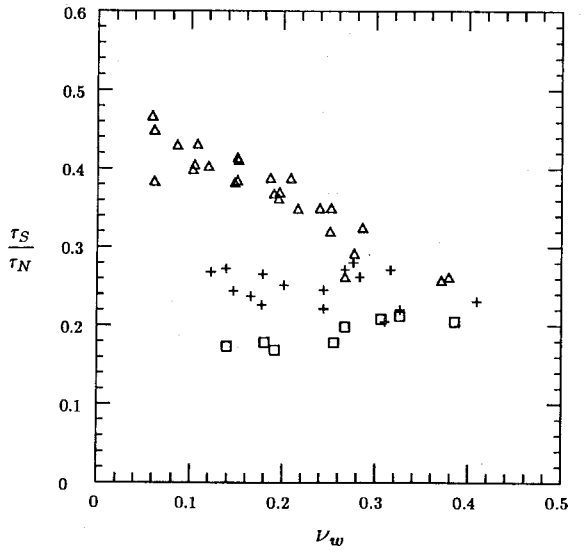

Fig. 9 Friction coefficient at the wall, $f = \tau_S/\tau_N$, against wall solid fraction, ν_w. □, the smooth surface; +, the moderately smooth surface; Δ, the rubberized surface.

the wall. The ratio of u'_w to u_w for the rubberized surface is larger than that for the smooth surface. The ratio u'_w/u_w for the smooth surface shows little variation with ν_w. For the moderately smooth surface, u'_w/u_w changes only mildly with ν_w. However, the rubberized surface clearly shows the increase of u'_w/u_w with decreasing ν_w.

5.2 Experimental Data on Friction Coefficient. As previously mentioned, shear stress was directly measured by the shear gauge, and normal stress was calculated as $\rho_p \nu_m g h \cos\theta$ where ρ_p is the density of particles, g is the gravitational acceleration, h is the depth of flow, and θ is the angle of the chute inclination. Note both stresses were measured at the chute base wall. Recall from Section 3 that kinematic Coulombic friction coefficients, μ_c, were measured for each surface condition; 0.15 for the smooth surface, 0.22 for the moderately smooth surface, and 0.38 for the rubberized surface.

The ratio of shear stress to normal stress, or friction coefficient, f, is plotted against wall solid fraction in Fig. 9. For

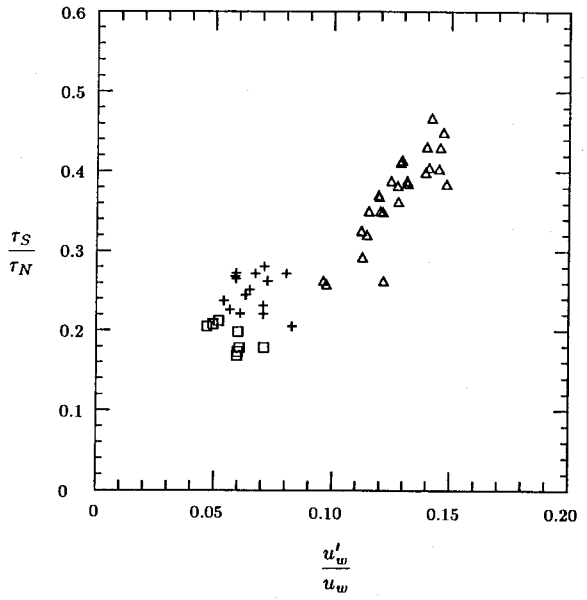

Fig. 10 Friction coefficient at the wall, $f = \tau_S/\tau_N$, against longitudinal velocity fluctuation at the wall normalized by mean velocity, u'_w/u_w. □, the smooth surface; +, the moderately smooth surface; Δ, the rubberized surface.

the smooth and moderately smooth surfaces, friction coefficients appear to be fairly constant. Furthermore, the values of friction coefficients are comparable to the kinematic Coulombic friction coefficients for each surface (though f is slightly higher than μ_c). On the other hand, for the rubberized surface, the friction coefficient is a decreasing function of solid fraction. And the Coulombic friction coefficient for the rubberized surface does not seem to directly affect the friction coefficient for the flowing material. Therefore, it may be concluded that the different surface conditions result in quite different types of boundary condition at the wall.

In Fig. 10, the friction coefficient is plotted against velocity fluctuation normalized by mean velocity, or u'_w/u_w. For the smooth and moderately smooth surfaces, all the data are clustered at one region. For the rubberized surface, f seems to correlate quite well with u'_w/u_w; f increases with increasing u'_w/u_w. This phenomenon is independent of particle size.

5.3 Experimental Results on Rheological Behavior. The data on the normal and shear stresses will be examined by comparison with the rheological model of Lun et al. (1984). In particular we examine the stresses by normalizing by $\rho_p(u'_w)^2$ and $\rho_p(d\Delta u/h)u'_w$ (see equations (2) and (3), for any kind of flow). Other possible normalizing factors which merit investigation are $\rho_p(d\Delta u/h)^2$ (see equations (6) and (7), for simple shear flow), $\rho_p(d\Delta u/h)^2/\tan^2\theta$, and $\rho_p(d\Delta u/h)^2/\tan\theta$ (see equations (9) and (10), for fully developed flow). In this investigation, it is important to recall that Lun et al. assume that the granular temperature is isotropic, and that the effects of particle rotation and surface friction are not included in their model. One could, therefore, expect some discrepancies in comparison with the experimental data.

The theory of Lun et al. suggests that the appropriate normalizing factor of the normal stress should be $\rho_p(u'_w)^2$, and the experimental data thus normalized is plotted against the wall solid fraction in Fig. 11(*a*). This method of normalization appears to correlate the data quite well and seems to collapse the data for the different surface conditions. When these same values are plotted against the mean solid fraction as in Fig. 11(*b*), the data are more scattered. This may be explained by realizing that the normalized stress is a local quantity which should be related to the local wall solid fraction rather than the mean solid fraction. In both figures, results for the rheo-

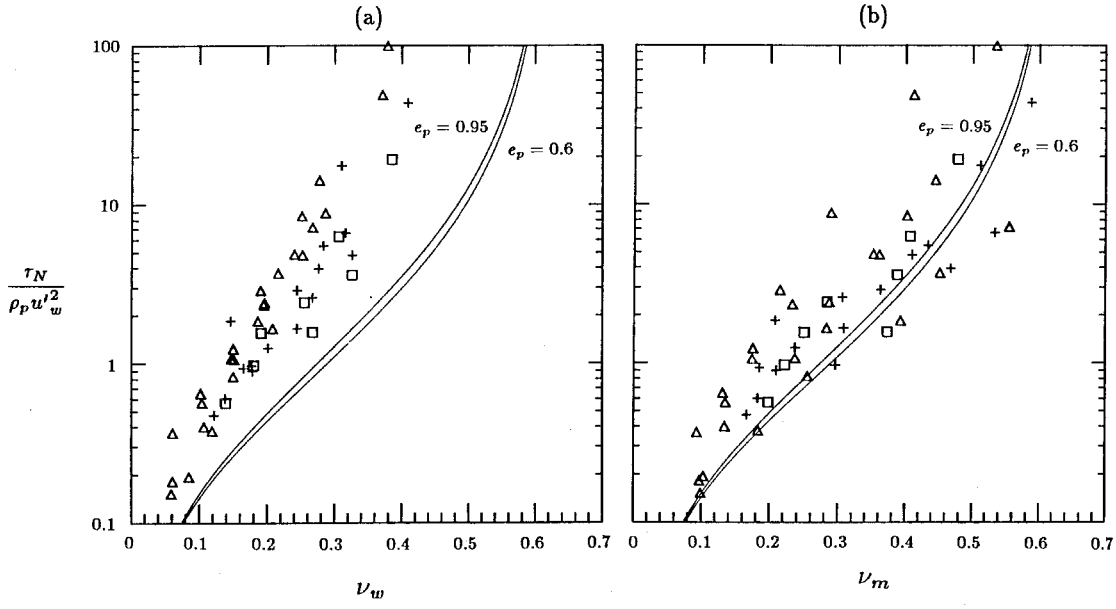

Fig. 11 The normalized normal stress, $\tau_N/\rho_p u'^2_w$, against (*a*) wall solid fraction, ν_w, and (*b*) mean solid fraction, ν_m. □, the smooth surface; +, the moderately smooth surface; Δ, the rubberized surface. The solid lines, the results of Lun et al. (1984).

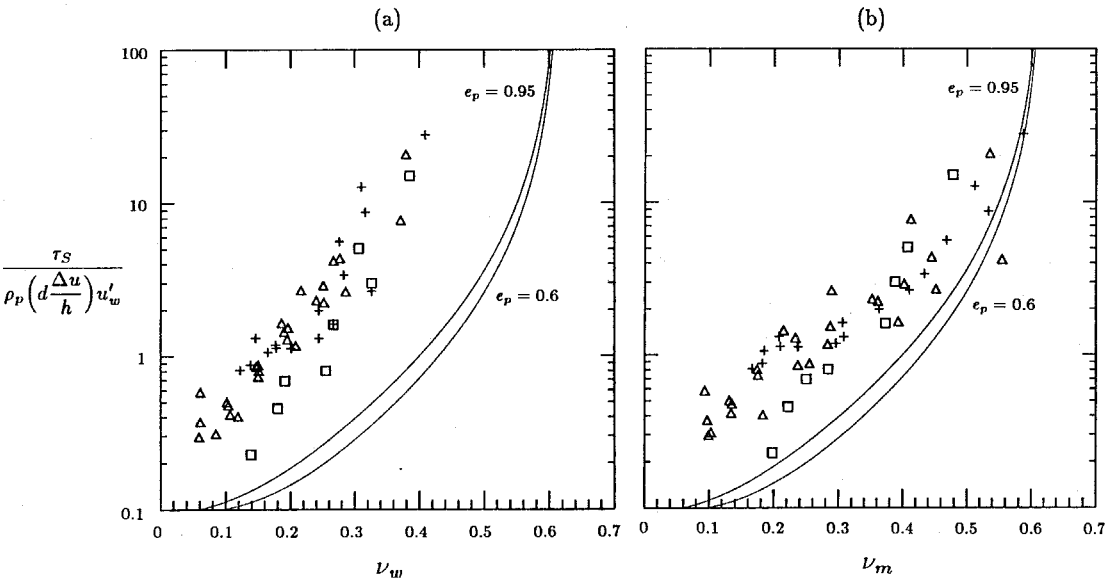

Fig. 12 The normalized shear stress, $\tau_S/\rho_p d(\Delta u/h)u'_w$, against (*a*) wall solid fraction, ν_w, and (*b*) mean solid fraction, ν_m. □, the smooth surface; +, the moderately smooth surface; Δ, the rubberized surface. The solid lines, the results of Lun et al. (1984).

logical model postulated by Lun et al. (1984) (see equation (2)) are also plotted using $T=\langle u'^2\rangle$.

On the other hand, the theory of Lun et al. suggests that the shear stress should be normalized by $\rho_p(d\Delta u/h)u'_w$, and the resulting experimental data is presented in Fig. 12. Again the data is well correlated regardless of surface conditions when plotted against the wall solid fraction, and the data is less satisfactorily correlated with the mean solid fraction. The results of Lun et al. (1984) for any general flow (see equation (3)) are shown in the same figure for comparison. The quantitative discrepancy between the theoretical and experimental results is substantial.

It should also be observed that alternative normalizations with $\rho_p(d\Delta u/h)^2$, $\rho_p(d\Delta u/h)^2/\tan^2\theta$, and $\rho_p(d\Delta u/h)^2/\tan\theta$ yielded less satisfactory correlation of the data than in Figs. 11(*a*) and 12(*a*) (see Ahn (1989)). This strongly implies that the rheological models of Lun et al. have considerable merit in so far as the functional dependence on the flow parameter is concerned though the quantitative values of some of the coefficients may be significantly in error.

We now examine the parameter, S, introduced by Savage and Jeffrey (1981) where

$$S=\frac{d\dfrac{du}{dy}}{T^{1/2}}.$$

The model of Lun et al. (1984) predicts that S should be a function only of ν and e_p for simple shear flow and that $S/\tan\theta$ should likewise be a function only of ν and e_p in fully

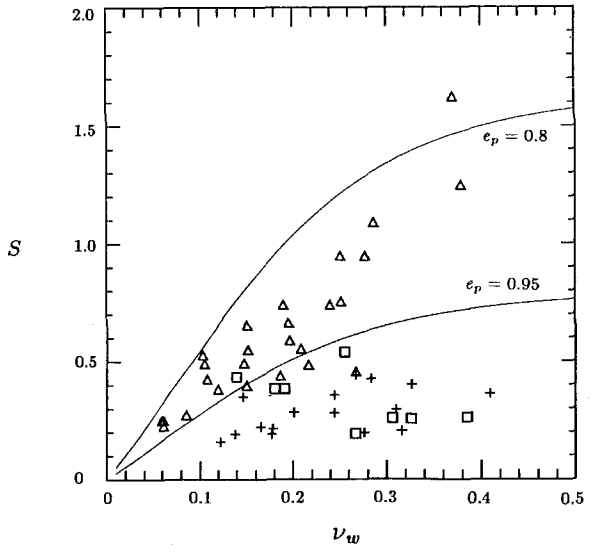

Fig. 13 The parameter, $S = d(\Delta u/h)/u'_w$, against wall solid fraction, ν_w. □, the smooth surface; +, the moderately smooth surface; Δ, the rubberized surface. The solid lines, the results of Lun et al. (1984).

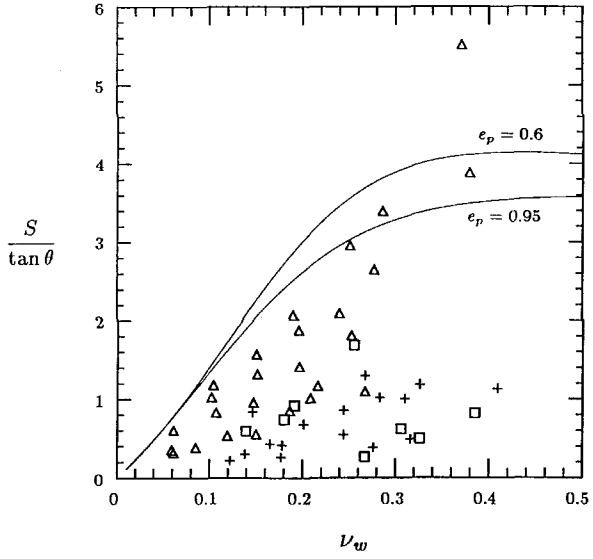

Fig. 14 The parameter, $S/\tan\theta = d(\Delta u/h)u'_w \tan\theta$, against wall solid fraction, ν_w. □, the smooth surface; +, the moderately smooth surface; Δ, the rubberized surface. The solid lines, the results of Lun et al. (1984).

developed flow (see equations (5) and (8)). Here we estimate S by $d(\Delta u/h)/u'_w$. The parameter S is plotted against the wall solid fraction in Fig. 13 while $S/\tan\theta$ is presented in Fig. 14. In both figures the data is widely scattered showing strong dependency on surface conditions. We believe, for reasons stated later, that this is due to the fact that the flow is not a simple shear flow and that only a subset of the data represent fully developed flows.

6 Discussion

6.1 The Characteristics of Chute Flows. It is apparent from Fig. 5 that the surface condition has considerable influence on the characteristics of chute flow. Different results have been achieved by several authors when different surface conditions are used. For example, Bailard (1978) used a surface on which grains were glued, and Savage (1979) applied roughened rubber sheets to the surface. In both cases, the ratio of u_w to u_s was close to zero. Augenstein and Hogg (1978) obtained various u_w/u_s for various surface roughnesses. When a smooth surface with high friction coefficient was used by Campbell and Brennen (1985b) in computer simulations, the ratio of u_w to u_s was about $0.4 \sim 0.5$. The rubberized surface of the present experiments, therefore, is similar to those cases in Campbell and Brennen in which a no-slip condition at the contact surface was assumed. Despite these data, the present state of knowledge does not allow prediction of the slip at the wall. Indeed, the features of the surface or of the flow which determine the slip are not well understood.

The surface conditions also influence velocity fluctuations at the wall as observed in Fig. 8. For the smooth and moderately smooth surfaces, the ratio of u'_w to u_w is low and fairly constant. On the other hand, u'_w/u_w for the rubberized surface is high and increases as solid fraction decreases. These observations may imply the following. The rubberized surface is characterized by large velocity fluctuations particularly at lower solid fractions. The high fluctuations and the low solid fraction allow particles to move more freely from one location to another. One of the effects by these random motions is a decrease of velocity gradient in the direction normal to the flow. That is, when particles move from a layer with low mean velocity to a subsequent layer with high velocity, the mean velocity of the layer with high velocity is reduced. When particles move due to random motion from the upper layer with high mean velocity to the lower layer with low mean velocity, the opposite is true. This phenomenon is consistent with experimental observations. For the rubberized surface, u_w/u_s rather sharply increases at $\nu \simeq 0.1$ as the solid fraction is decreased (see Fig. 5). As also observed in Fig. 6(*c*), since at low solid fraction velocity fluctuation is high and there is more space for particles to freely move, the shear rate decreases as solid fraction decreases. In Fig. 6(*a*), however, this decrease of the shear rate is not observed with the smooth surface since no substantial velocity fluctuation exists (see Fig. 8).

6.2 Friction Coefficient and Boundary Conditions. In the present work, an attempt to investigate boundary conditions was made by changing chute surface conditions. The Coulombic friction coefficient, μ_c, was measured for each surface since it was anticipated that μ_c would be a major factor which determines whether or not particles slip when in contact with solid boundary. Here the word "slip" means the tangential slip between the contact surfaces of the particle and the wall. The slip velocity is different from a velocity at the wall, u_w, which is the velocity of the particle center extrapolated to the wall. Clearly, even when slip velocity is zero, a particle touching the wall may roll and thus have a nonzero center velocity.

When a particle collides with a wall such that the shear stress at the contact point exceeds a shear stress limit which the surface can withstand for the given normal stress at the contact point, slip will occur. Then the ratio of the shear stress to the normal stress at the contact point is adjusted to the Coulombic friction coefficient of the surface, i.e. $f = \mu_c$. On the other hand, when the ratio of τ_S to τ_N at the impact does not exceed μ_c, there will be no slip between the contact surfaces of the particle and the wall. In this case f is different from μ_c.

As seen in Fig. 9, friction coefficients for the smooth and moderately smooth surfaces seem to be fairly constant. But for the rubberized surface the friction coefficient decreases with increasing solid fraction. Decreasing friction coefficients with increasing ν were also observed in the shear cell experiments of Savage and Sayed (1984) and in the computer simulations of Campbell (1989). However, the constant friction coefficients of the smooth and moderately smooth surfaces have not been observed previously. To explain these observations, we suggest the following. For the smooth and moderately smooth surfaces, slip occurs at the contact between particles and the surfaces, and the slip condition results in the

constant friction coefficient equal to μ_c. On the other hand, the varying friction coefficient for the rubberized surface suggests a no-slip condition at the boundary. The high Coulombic friction coefficient of the rubberized surface would inhibit any slip at the contact between particles and the surface.

When there is no slip, the following relation results from a simple analysis of the oblique impact of a single sphere on the flat surface (see Ahn (1989)):

$$f=\frac{2}{7}\left(1-\frac{\omega_1 r}{u_1}\right)\frac{\tan\alpha_1}{1+e_w}$$

where ω_1 is the rotational rate before impact, r is the radius of the sphere, and u_1 is the velocity tangential to the wall before impact. The impact angle α_1 is defined by $\tan^{-1}(u_1/v_1)$ where v_1 is the velocity normal to the wall before impact, and e_w is the wall-particle coefficient of restitution. In this equation, the friction coefficient or the ratio of τ_S to τ_N at the surface depends on the ratio of rotational velocity to tangential velocity, $\omega_1 r/u_1$, and on the impact angle, $\tan\alpha_1$.

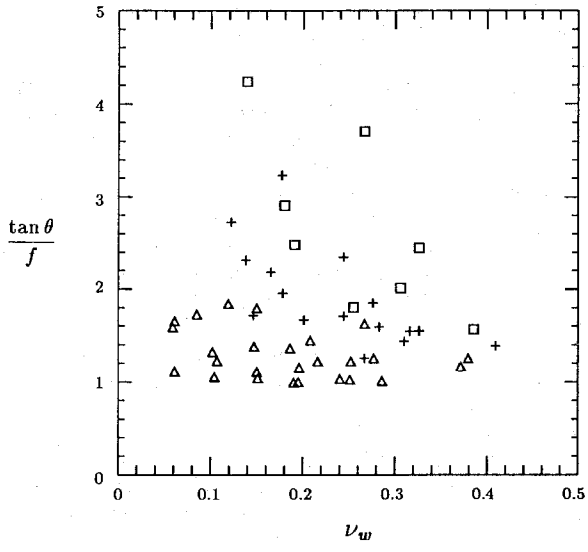

Fig. 15 The ratio of tan θ to f against wall solid fraction, ν_w. □, the smooth surface; +, the moderately smooth surface; Δ, the rubberized surface.

In the present experiments, the values of $\tan\alpha_1$ could not be estimated. Another factor influencing f is the ratio of the rotational velocity ωr to the tangential velocity u before impact. Campbell (1988) has shown that next to the wall ω is considerably larger than the mean value, but that with a small distance from the wall ω is slightly less than the mean value. Therefore, when a particle next to the wall with high ω hits the wall, the friction coefficient will be low, but if a particle at a distance from the wall with low ω comes down and collides with the wall, the friction coefficient will be relatively high.

These phenomena suggests a possible explanation for the decrease in the friction coefficient as the solid fraction increases. At low solid fraction particles move more freely from one layer to another. Thus more particles in the upper layer with small values of $\omega r/u$ move down to the boundary and make collisions with the wall. Because friction is measured in a statistical sense as a sum of frictions due to individual particles colliding with the wall, f is therefore high at low solid fraction. On the other hand, at high solid fraction and low granular temperature, very few particles in the upper layer with low $\omega r/u$ penetrate to the wall. As a result, particles next to the wall with high rotational velocity will dominate collisions at the wall. Thus, f would be smaller at high solid fraction.

This explanation appears to be consistent with the data for the rubberized surface where no slip is expected (see Fig. 9). The general trend of decreasing f with increasing ν holds independent of particle size. In Fig. 10, f is plotted against u'_w/u_w. When higher u'_w/u_w exists, particles with low ω in the upper layer more easily move down to the boundary and collide with the wall. That is, as u'_w/u_w increases, the intrusion of particles with low ω from the upper layer into the boundary becomes more frequent, causing f to increase. As a result, the friction coefficient appears to be a fairly linear function of u'_w/u_w for the rubberized surface.

For the smooth and moderately smooth surfaces, slip occurs and μ_c controls the boundary conditions. Therefore, f is comparable to μ_c (see Fig. 9), and f is unrelated to u'_w/u_w (see Fig. 10). (However, one might argue from Fig. 10 that for the smooth and moderately smooth surfaces f is small because u'_w/u_w is small. Then it appears that regardless of the surface conditions f has a fairly linear relation to u'_w/u_w).

6.3 Stresses and Rheological Behavior. When the experimental data on the normal and shear stresses are normalized in the same way as in the rheological models by Lun et al.

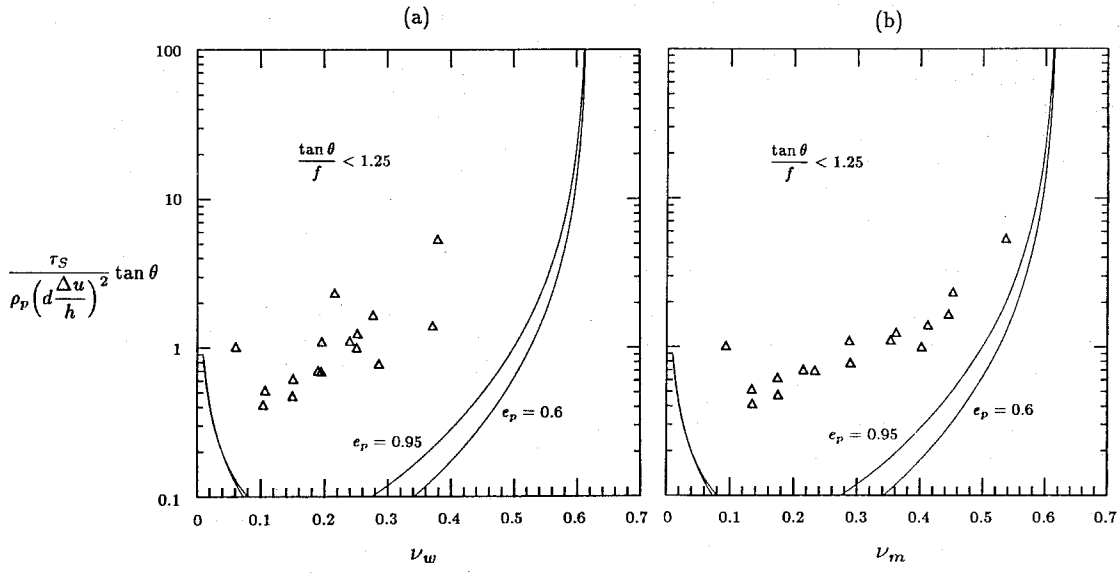

Fig. 16 The normalized shear stress, $\tau_S \tan\theta/\rho_p(d\Delta u/h)^2$, against (*a*) wall solid fraction, ν_w, and (*b*) mean solid fraction, ν_m. Data only with $\tan\theta/f<1.25$. The solid lines, the results of Lun et al. (1984).

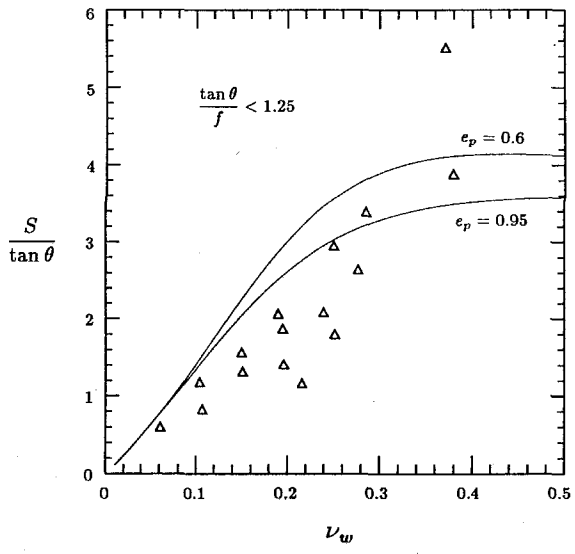

Fig. 17 The parameter, $S/\tan\theta = d(\Delta u/h)/u_w'$ tan θ, against wall solid fraction, ν_w. Data only with tan $\theta/f < 1.25$. The solid lines, the results of Lun et al. (1984).

(1984), the measurements turn out to be well correlated as shown in Figs. 11(*a*) and 12(*a*). (The models should hold for any flow whether fully developed flow or not.) The data are also internally consistent, independent of the surface boundary conditions. It is also important to note that other normalizations such as $\tau_N/\rho_p(d\Delta u/h)^2$ and $\tau_S/\rho_p(d\Delta u/h)^2$ (Ahn (1989)) do not lead to such satisfactory collapse of the data and yield curves which appear to depend on the surface boundary condition.

The chute flows in the present experiments were not fully developed. This is confirmed by comparing friction coefficient with the tangent value of the chute inclination angle. The ratio of tan θ to f is plotted in Fig. 15. If the flow were fully developed, the ratio would be 1, and the results clearly show that this is not the case. Therefore, when $\tau_N \tan^2\theta/\rho_p(d\Delta u/h)^2$ and $\tau_S \tan\theta/\rho_p(d\Delta u/h)^2$ are plotted against the wall solid fraction, ν_w, considerable scatter is observed since these correlations would only hold for fully developed flows. However, we can select those data points which represent nearly fully developed flow by applying the requirement that $\tan\theta/f < 1.25$ where the 1.25 is somewhat arbitrary. This subset of data is used to present the shear stress normalized by $\rho_p(d\Delta u/h)^2/\tan\theta$ in Fig. 16. It is significant that this subset of data is well correlated in this figure. Though not presented here, the normal stress normalized by $\rho_p(d\Delta u/h)^2/\tan^2\theta$ would also be well correlated when $\tan\theta/f < 1.25$. Furthermore, this subset of data is also used to present $S/\tan\theta$ in Fig. 17 in which the scatter is much less than in Fig. 14. This indicates again that the fully developed flows adhere to the model expected on the basis of the theory of Lun et al. (1984). On the other hand, it is clear that many of the chute flows examined here were not fully developed.

In summary, it may be concluded that the rheological models for general flow (equations (2) and (3)) give good correlation to the present experimental data (see Figs. 11 and 12). The rheological model for fully developed flow (equation (9) or (10)) also agrees with a subset of experimental data which is judged to be fully developed (see Fig. 16).

7 Summary and Conclusion

Experiments on continuous, steady flows of granular materials down an inclined chute have been made with the objectives of understanding the characteristics of chute flows, and of acquiring information on the rheological behavior of granular materials. Two neighboring fiber-optic displacement probes were used to measure mean velocity, one component of velocity fluctuations, and mean particle spacing. The mean particle spacing also gave qualitative information on density near the boundaries. In addition, a strain-gauged plate was employed to directly measure shear stress at the chute base. The surface of the chute base was carefully controlled to yield three distinct surface conditions; smooth aluminum surface; moderately smooth aluminum surface, rubber-coated surface. Each surface condition was characterized by Coulombic friction coefficient and the coefficient of restitution between the chute base and a particle.

The preliminary experiments indicate that the flow at the free surface is less affected by the sidewalls than at the chute base; the transverse velocity profile at the free surface is close to uniform. It is also observed that the higher the velocity (or the higher the chute inclination), the less significant the sidewall effect.

Vertical profiles of velocity, velocity fluctuation, and linear concentration have been measured through lucite windows in the sidewalls. The velocity profile is fairly linear except for the region within the distance of one particle diameter from the chute base. Velocity fluctuation increases with distance from the chute base. This granular conduction from the bulk of the flow to the chute base wall is opposite to what we observe from the results of Campbell and Brennen (1985b). The results of Ahn et al. (1989) indicate that granular temperature can be conducted in either direction, depending on the value of the particle-particle coefficient of restitution and the chute inclination. In the present measurements, linear concentration always decreases monotonically with distance from the chute base. This result is also different from the results found in the other literature. The surface condition of the chute base plays an important role in the above profiles. The profiles of velocity and its fluctuation with the smooth surface (the surface with low Coulombic friction coefficient) are more uniform than those with the rubber-coated surface (the surface with high Coulombic friction coefficient).

The characteristics of the chute flow of granular materials have been studied by measuring various basic flow properties. The experimental data are strongly affected by the surface condition of the chute base. The ratio of velocity fluctuation to mean velocity is fairly constant for the smooth and moderately smooth surfaces, but for the rubberized surface it clearly increases as the solid fraction decreases. And the ratio for the rubberized surface is much larger than those for the smooth and moderately smooth surfaces. Regardless of the surface conditions, the mean shear rate increases at high solid fraction with decreasing solid fraction. But for the rubberized surface the mean shear rate shows a drastic decrease at low solid fraction. The high ratio of velocity fluctuation to mean velocity causes particles to move from one location to another more frequently, and as a result the velocity gradient is reduced. For the smooth surface where the ratio is low, the decrease of mean shear rate is not observed with decreasing solid fraction.

The variation of friction coefficient with solid fraction is similar to that of the ratio of velocity fluctuation to mean velocity. For the smooth and moderately smooth surfaces, the friction coefficient is fairly constant. But for the rubberized surface, it increases with decreasing solid fraction. As a result, the friction coefficient appears to be a linear function of the ratio of velocity fluctuation to mean velocity.

The stress measurements have also been used to study the rheological behavior of granular material. In particular, the rheological models presented by Lun et al. (1984) have been compared. The rheological models for general flow (equations (2) and (3)) give good correlation to the present experimental data. With the smooth and moderately smooth surfaces, it was not possible to create fully developed flow. But some selected experimental data with the rubberized surface, which are close

to fully developed flow, are well correlated with the rheological models for fully developed flow (equations (9) or (10)). Since the chute flows of the present experiments are characterized by granular conduction, the rheological models for simple shear flow (equations (6) and (7)) do not provide good correlation for the present experimental data.

References

Ahn, H., 1989, "Experimental and Analytical Investigations of Granular Materials: Shear Flow and Convective Heat Transfer," Ph.D. Thesis, California Institute of Technology, Pasadena, Calif.

Ahn, H., Brennen, C. E., and Sabersky, R. H., 1988, "Experiments on Chute Flows of Granular Materials," *Micromechanics of Granular Materials*, (M. Satake and J. T. Jenkins, eds.), Elsevier, Amsterdam, pp. 339–348.

Ahn, H., Brennen, C. E., and Sabersky, R. H., 1989, "Analysis of the Fully Developed Chute Flow of Granular Materials," submitted to ASME JOURNAL OF APPLIED MECHANICS.

Augenstein, D. A., and Hogg, R., 1978, "An Experimental Study of the Flow of Dry Powders on Inclined Surfaces," *Powder Technology*, Vol. 19, pp. 205–215.

Bagnold, R. A., 1954, "Experiments on a Gravity-Free Dispersion of Large Solid Particles in a Newtonian Fluid Under Shear," *Proc. R. Soc. Lond.*, Vol. A225, pp. 49–63.

Bailard, J., 1978, "An Experimental Study of Granular-Fluid Flow," Ph.D. Thesis, University of California, San Diego, Calif.

Campbell, C. S., 1982, "Shear Flow of Granular Materials," Ph.D. Thesis, California Institute of Technology, Pasadena, Calif.

Campbell, C. S., 1986, "The Effect of Microstructure Development on the Collisional Stress Tensor in a Granular Flow," *Acta Mechanica*, Vol. 63, pp. 61–72.

Campbell, C. S., 1988, "Boundary Interactions for Two-Dimensional Granular Flows: Asymmetric Stresses and Couple Stresses," *Micromechanics of Granular Materials*, M. Satake and J. T. Jenkins, eds., Elsevier, Amsterdam, pp. 163–174.

Campbell, C. S., 1989, "The Stress Tensor for Simple Shear Flows of a Granular Material," *J. Fluid Mech.*, to be published.

Campbell, C. S., and Brennen, C. E., 1985a, "Computer Simulation of Granular Shear Flows," *J. Fluid Mech.*, Vol. 151, pp. 167–188.

Campbell, C. S., and Brennen, C. E., 1985b, "Chute Flows of Granular Material: Some Computer Simulation," ASME JOURNAL OF APPLIED MECHANICS, Vol. 52, pp. 172–178.

Campbell, C. S., and Gong, A., 1986, "The Stress Tensor in a Two-Dimensional Granular Shear Flow," *J. Fluid Mech.*, Vol. 164, pp. 107–125.

Campbell, C. S., and Gong, A., 1987, "Boundary Conditions for Two-Dimensional Granular Flows," *Proceedings of the International Symposium on Multiphase Flows*, Vol. 1, Hangzhou, China, pp. 278–283.

Craig, K., Buckholz, R. H., and Domoto, G., 1986, "An Experimental Study of the Rapid Flow of Dry Cohesionless Metal Powders," ASME JOURNAL OF APPLIED MECHANICS, Vol. 53, pp. 935–942.

Hanes, D. M., and Inman, D. L., 1985, "Observations of Rapidly Flowing Granular-Fluid Flow," *J. Fluid Mech.*, Vol. 150, pp. 357–380.

Jenkins, J. T., and Savage, S. B., 1983, "A Theory for the Rapid Flow of Identical, Smooth, Nearly Elastic Particles," *J. Fluid Mech.*, Vol. 130, pp. 187–202.

Lun, C. K. K., and Savage, S. B., 1986, "The Effects of an Impact Velocity Dependent Coefficient of Restitution on Stresses Developed by Sheared Granular Materials," *Acta Mechanica*, Vol. 63, pp. 15–44.

Lun, C. K. K., Savage, S. B., Jeffrey, D. J., and Chepurniy, N., 1984, "Kinetic Theories for Granular Flow: Inelastic Particles in Couette Flow and Slightly Inelastic Particles in a General Flow field," *J. Fluid Mech.*, Vol. 140, pp. 223–256.

Ogawa, S., Umemura, A., and Oshima, N., 1980, "On the Equations of Fully Fluidized Granular Materials," *J. Appl. Math. Phys.*, (ZAMP), Vol. 31, pp. 483–493.

Patton, J. S., 1985, "Experimental Study of Shear Flows and Convective Heat Transfer Characteristics of Granular Materials," Ph.D. Thesis, California Institute of Technology, Pasadena, Calif.

Patton, J. S., Brennen, C. E., and Sabersky, R. H., 1987, "Shear Flows of Rapidly Flowing Granular Materials," ASME JOURNAL OF APPLIED MECHANICS, Vol. 54, pp. 801–805.

Savage, S. B., 1979, "Gravity Flow of Cohesionless Granular Materials in Chutes and Channels," *J. Fluid Mech.*, Vol. 92, pp. 53–96.

Savage, S. B., 1984, "The Mechanics of Rapid Granular Flows," *Advances in Applied Mechanics*, Vol. 24, J. Hutchinson and T. Y. Wu, eds., Academic Press, pp. 289–366.

Savage, S. B., and Jeffrey, D. J., 1981, "The Stress Tensor in a Granular Flow at High Shear Rates," *J. Fluid Mech.*, Vol. 110, pp. 255–272.

Savage, S. B., and McKeown, S., 1983, "Shear Stress Developed During Rapid Shear of Dense Concentrations of Large Spherical Particles Between Concentric Cylinders," *J. Fluid Mech.*, Vol. 127, pp. 453–472.

Savage, S. B., and Sayed, M., 1984, "Stresses Developed by Dry Cohesionless Granular Materials in an Annular Shear Cell," *J. Fluid Mech.*, Vol. 142, pp. 391–430.

Sayed, M., and Savage, S. B., 1983, "Rapid Gravity Flow of Cohesionless Granular Materials Down Inclined Chutes," *J. Appl. Math. Phys.*, Vol. 34, pp. 84–100.

Walton, O. R., 1984, "Computer Simulation of Particulate Flow," *Energy and Tech. Rev.*, Lawrence Livermore Lab., May 1984, p. 24.

Walton, O. R., and Braun, R. L., 1986a, "Viscosity, Granular-Temperature, and Stress Calculations for Shearing Assemblies of Inelastic, Frictional Disks," *J. of Rheology*, Vol. 30, No. 5, pp. 949–980.

Walton, O. R., and Braun, R. L., 1986b, "Stress Calculations for Assemblies of Inelastic Spheres in Uniform Shear," *Acta Mechanica*, Vol. 63, pp. 73–86.